



## Data Article

# Proteomics dataset of lysolecithin-induced demyelinated lesions in corpus callosum of Lewis rats, treated with Vagus nerve stimulation or sham treatment



Helen Bachmann<sup>a,\*</sup>, Boris Vandemoortele<sup>b,c,d</sup>,  
Vanessa Vermeirssen<sup>b,c,d</sup>, Evelien Carrette<sup>a</sup>, Kristl Vonck<sup>a</sup>,  
Paul Boon<sup>a</sup>, Robrecht Raedt<sup>a,1</sup>, Guy Laureys<sup>a,1</sup>

<sup>a</sup> *4Brain, Department of Neurology, Ghent University, Ghent University Hospital, Corneel Heymanslaan 10, 9000 Ghent, Belgium*

<sup>b</sup> *Laboratory for Computational Biology, Integromics and Gene Regulation (CBIGR), Cancer Research Institute Ghent (CRIG), Corneel Heymanslaan 10, 9000 Ghent, Belgium*

<sup>c</sup> *Department of Biomedical Molecular Biology, Ghent University, Zwijnaarde-Technologiepark 71, 9000 Ghent, Belgium*

<sup>d</sup> *Department of Biomolecular Medicine, Ghent University, Corneel Heymanslaan 10, 9000 Ghent, Belgium*

## ARTICLE INFO

## Article history:

Received 15 May 2024

Revised 4 October 2024

Accepted 11 October 2024

Available online 18 October 2024

Dataset link: [PXD050858 \(Original data\)](https://doi.org/10.1016/j.dib.2024.111048)

## Keywords:

Proteomics

Demyelination

Lysolecithin

Corpus callosum

Vagus Nerve Stimulation

Rat

## ABSTRACT

This article presents a comprehensive proteomics dataset from a lysolecithin (LPC)-induced demyelination model in the corpus callosum of female Lewis rats. The LPC model, widely used in preclinical studies of toxic demyelination, serves as a valuable tool for investigating processes of demyelination and remyelination, as well as for testing potential remyelination therapies for diseases like Multiple Sclerosis. In this study, rats received either Vagus Nerve Stimulation (VNS) or a sham treatment. Proteomic analysis via LC-MS/MS was performed to assess the impact of these treatments on inflammation and remyelination and to further explore the mechanism of VNS action. This dataset complements the findings reported in the article “*Vagus Nerve Stimulation enhances remyelination and decreases innate neuroinflammation in lysolecithin-induced demyelination*” [1], providing a detailed account of the pro-

\* Corresponding author.

E-mail address: [Helen.Bachmann@UGent.be](mailto:Helen.Bachmann@UGent.be) (H. Bachmann).

<sup>1</sup> Shared senior authorship

teomics methods and results, including the quantification of 8172 proteins. This dataset allows for further exploration of key mechanisms in the LPC model by comparing different time points within the sham group. Additionally, comparisons between the sham and VNS groups can be extended or combined with other published datasets to gain deeper insights into the effects of VNS. Raw data are available via ProteomeXchange with identifier PXD050858.

© 2024 The Authors. Published by Elsevier Inc.

This is an open access article under the CC BY-NC license (<http://creativecommons.org/licenses/by-nc/4.0/>)

## Specifications Table

Subject	Biological Sciences: Proteomics
Specific subject area	Mass spectrometry data, tables with identified proteins, tables with differentially expressed proteins, data analysis scripts
Type of data	Table, Figures Raw, Analyzed Data analysis scripts
Data collection	Brain tissue of Lewis rats, containing demyelinated lesion in the corpus callosum, was collected at 3 days or 11 days post-lesioning, after treatment by either VNS or sham. Five replicates per condition were selected for lesion sampling, of which protein content was extracted and analyzed by LC-MS/MS. Raw LC-MS/MS files were made publicly available within the ProteomeXchange Consortium.
Data source location	Ghent University, 4Brain, Department of Neurology, Ghent University Hospital Ghent, Belgium
Data accessibility	Mass spectrometry data have been deposited to the ProteomeXchange Consortium via the Proteomics Identifications Database (PRIDE) repository with dataset identification number PXD050858. This data can be accessed via <a href="http://www.ebi.ac.uk/pride">http://www.ebi.ac.uk/pride</a> using the accession number PXD050858. Data DOI: <a href="https://doi.org/10.1016/J.BRS.2024.04.012">10.1016/J.BRS.2024.04.012</a> Data URL: <a href="https://www.ebi.ac.uk/pride/archive/projects/PXD050858">https://www.ebi.ac.uk/pride/archive/projects/PXD050858</a> The data analyses scripts are deposited at GitHub. This data can be accessed via <a href="https://github.com/CBIGR/Lysolecithin_vagus_nerve_stimulation">https://github.com/CBIGR/Lysolecithin_vagus_nerve_stimulation</a> Data URL: <a href="https://github.com/CBIGR/Lysolecithin_vagus_nerve_stimulation">https://github.com/CBIGR/Lysolecithin_vagus_nerve_stimulation</a> The supplementary data including the identified and quantified protein lists, and the differential expression analyses are deposited at Zenodo (Supplementary_data.zip). The data analyses scripts are also deposited at Zenodo (CBIGR/Lysolecithin_vagus_nerve_stimulation-Version_1.zip). This data can be accessed via <a href="https://zenodo.org/records/13691679">https://zenodo.org/records/13691679</a> Data DOI: <a href="https://doi.org/10.5281/zenodo.12747993">10.5281/zenodo.12747993</a> Data URL: <a href="https://zenodo.org/records/13691679">https://zenodo.org/records/13691679</a>
Related research article	Bachmann, H., Vandemoortele, B., Vermeirssen, V., Carrette, E., Vonck, K., Boon, P., Raedt, R., & Laureys, G. (2024). Vagus nerve stimulation enhances remyelination and decreases innate neuroinflammation in lysolecithin-induced demyelination. <i>Brain stimulation</i> , 17(3), 575–587. Article DOI: <a href="https://doi.org/10.1016/j.brs.2024.04.012">https://doi.org/10.1016/j.brs.2024.04.012</a>

## 1. Value of the Data

- This high-resolution mass spectroscopy-based proteomics data (LC-MS/MS) is of importance because it delivers proteins that are up- or downregulated in the lysolecithin (LPC) toxic demyelination model in female Lewis rats, an experimental model used for investigating de- and remyelination processes of the central nervous system.

- This dataset, particularly of the sham animals, can be used to investigate the regulation of inflammatory and neurologically relevant proteins during the demyelination and the remyelination timepoints of the LPC model.
- Investigating the pathophysiology of LPC-induced demyelination helps to optimize experimental design when using this model, and supports research on the key mechanisms of endogenous lesion repair in the central nervous system.
- The dataset can also be pooled or compared with other proteomics data of experiments involving either LPC-induced demyelination or Vagus Nerve Stimulation treatment in rats.

## 2. Background

Proteomics (LC-MS/MS) analysis was conducted as part of a study investigating the effects of Vagus Nerve Stimulation (VNS) on lysolecithin (LPC)-induced demyelination [1], a well-established preclinical model for studying demyelination and remyelination processes relevant to Multiple Sclerosis (MS). In MS, demyelination of the central nervous system is driven by autoimmune-mediated inflammation, whereas in the LPC model, myelin loss is triggered by the direct gliotoxic effects of LPC on oligodendrocytes. This detergent-like action leads to oligodendrocyte death, myelin degradation, and secondary inflammation mediated by the activation of microglia and astrocytes via damage-associated molecular patterns. Subsequently, spontaneous remyelination occurs through oligodendrocyte precursor cells (OPCs) in a predictable timeline, making this model highly suitable for studying remyelination mechanisms and testing the effects of therapeutic interventions at specific time points [2]. In this study, female Lewis rats received LPC injections into the corpus callosum, and the resulting lesions were analyzed at 3 and 11 days post-injection (dpi). The rats were treated with either sham or continuous VNS (cVNS), with the aim of promoting remyelination and reducing neuroinflammation [3]. The cVNS protocol was based on previous studies demonstrating its central modulatory effects and the associated increase in norepinephrine levels in the brain, without inducing hypothermia [4]. The proteomic analysis compared the differential expression of proteins between the VNS and sham groups, as well as between the 3 dpi and 11 dpi timepoints. These timepoints represent key stages of the demyelination process: 3 dpi marks complete demyelination and peak inflammation, while 11 dpi represents the stage of partial remyelination. This provided insights into protein regulation during both acute demyelination and the remyelination phase [5–7]. The article offers a detailed description of the proteomics methodology, dataset, and the results of differential expression analyses, making the data accessible to researchers for further exploration and facilitating its use in future VNS or LPC studies.

## 3. Data Description

This current data article describes the proteomics data comparing the effect of VNS versus sham on LPC-induced lesions at either demyelination or remyelination, with five replicates for each condition. LC-MS/MS runs of all samples were searched together using the DiaNN algorithm (version 1.8.1) with mainly default search settings, including a false discovery rate set at 1 % on precursor and protein level. Spectra were searched against the *Rattus norvegicus* (TaxID: 10116) protein sequences in the Uniprot database (database release version of 06\_2023), containing 47,942 sequences ([www.uniprot.org](http://www.uniprot.org)).

The raw data are deposited to the PRIDE depository with accession number PXD050858 (<https://www.ebi.ac.uk/pride/archive/projects/PXD050858>).

The folder **T03219\_EvoAurEI3\_20SPDDIAPASEF-PRC-6146\_1\_S1-F1\_1\_3564** contains the raw data of sham demyelination replicate 1, and analogously the other folders contain the raw data of the other replicates and experimental conditions, as shown in [Table 1](#). The folders **remyelination**, **demyelination**, **cVNS**, **sham** and **Output\_all** contain the reports (**report.tsv**, **report.pdf**, **report.auto.pipeline**, **report.pg\_matrix.tsv**, **report.pr\_matrix.tsv**, **report.stats.tsv**,

**Table 1**  
Raw data folders on PRIDE depository.

Folder name	Replicate
T03219_EvoAurEI3_20SPDDIAPASEF-PRC-6146_1_S1-F1_1_3564	Sham demyelination replicate 1
T03220_EvoAurEI3_20SPDDIAPASEF-PRC-6146_2_S1-F2_1_3565	Sham demyelination replicate 2
T03221_EvoAurEI3_20SPDDIAPASEF-PRC-6146_3_S1-F3_1_3566	Sham demyelination replicate 3
T03222_EvoAurEI3_20SPDDIAPASEF-PRC-6146_4_S1-F4_1_3567	Sham demyelination replicate 4
T03223_EvoAurEI3_20SPDDIAPASEF-PRC-6146_5_S1-F5_1_3568	Sham demyelination replicate 5
T03224_EvoAurEI3_20SPDDIAPASEF-PRC-6146_6_S1-F6_1_3569	cVNS demyelination replicate 1
T03225_EvoAurEI3_20SPDDIAPASEF-PRC-6146_7_S1-F7_1_3570	cVNS demyelination replicate 2
T03226_EvoAurEI3_20SPDDIAPASEF-PRC-6146_8_S1-F8_1_3571	cVNS demyelination replicate 3
T03227_EvoAurEI3_20SPDDIAPASEF-PRC-6146_9_S1-F9_1_3572	cVNS demyelination replicate 4
T03228_EvoAurEI3_20SPDDIAPASEF-PRC-6146_10_S1-F10_1_3573	cVNS demyelination replicate 5
T03229_EvoAurEI3_20SPDDIAPASEF-PRC-6146_11_S1-F11_1_3574	Sham remyelination replicate 1
T03230_EvoAurEI3_20SPDDIAPASEF-PRC-6146_12_S1-F12_1_3575	Sham remyelination replicate 2
T03231_EvoAurEI3_20SPDDIAPASEF-PRC-6146_13_S1-G1_1_3576	Sham remyelination replicate 3
T03232_EvoAurEI3_20SPDDIAPASEF-PRC-6146_14_S1-G2_1_3577	Sham remyelination replicate 4
T03233_EvoAurEI3_20SPDDIAPASEF-PRC-6146_15_S1-G3_1_3578	Sham remyelination replicate 5
T03234_EvoAurEI3_20SPDDIAPASEF-PRC-6146_16_S1-G4_1_3579	cVNS remyelination replicate 1
T03235_EvoAurEI3_20SPDDIAPASEF-PRC-6146_17_S1-G5_1_3580	cVNS remyelination replicate 2
T03236_EvoAurEI3_20SPDDIAPASEF-PRC-6146_18_S1-G6_1_3581	cVNS remyelination replicate 3
T03237_EvoAurEI3_20SPDDIAPASEF-PRC-6146_19_S1-G7_1_3582	cVNS remyelination replicate 4
T03238_EvoAurEI3_20SPDDIAPASEF-PRC-6146_20_S1-G8_1_3583	cVNS remyelination replicate 5

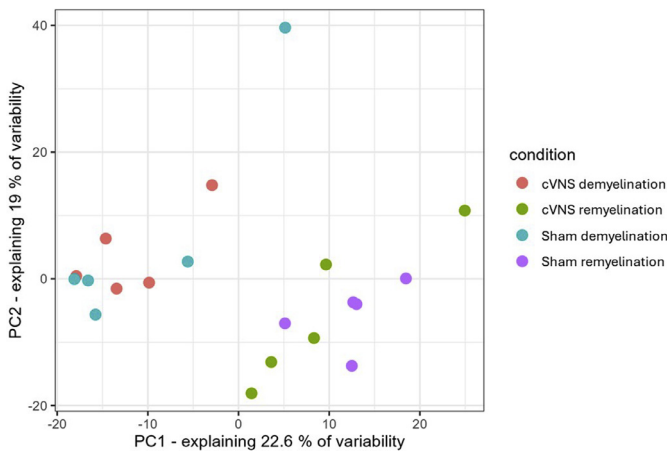


**Fig. 1.** Scatter plot representing the principal component analysis of the 8172 reliable quantified proteins ( $\geq 3$  valid PG.MaxLFQ valid values in  $\geq 1$  experimental condition) ( $n = 20$ ). The scatter plot shows sample projections along the first two principal components (PCs). Percentages of explained data variance for each PC are shown on the X-and Y-axis. Samples were colored by treatment group.

**report.unique\_genes\_matrix.tsv, report-first-pass.tsv, report-first-pass.gg\_matrix.tsv, report-first-pass.pg\_matrix.tsv, report-first-pass.pr\_matrix.tsv, report-first-pass.stats.tsv, report-first-pass.unique\_genes\_matrix.tsv**), and output library (**outputLib, outputLib.speclib**) of each experimental condition.

The identified and quantified protein lists, differential expression analyses, and data analyses scripts are deposited at Zenodo (<https://zenodo.org/records/12749816>).

In all samples, 8271 proteins were identified, listed in **Identified\_Proteins.xlsx**, in which they are sorted by protein abundance (iBAQ values). Of these, 8172 proteins were reliably quantified, if they had at least 3 valid PG.MaxLFQ values in one of the experimental conditions, listed in **Quantified\_Proteins.xlsx**. A Principal Component Analysis (PCA) was performed on the replicate samples using all quantified proteins as variables, shown in **Fig. 1**. A heatmap of sample correlations after hierarchical clustering is shown in **Fig. 2**.

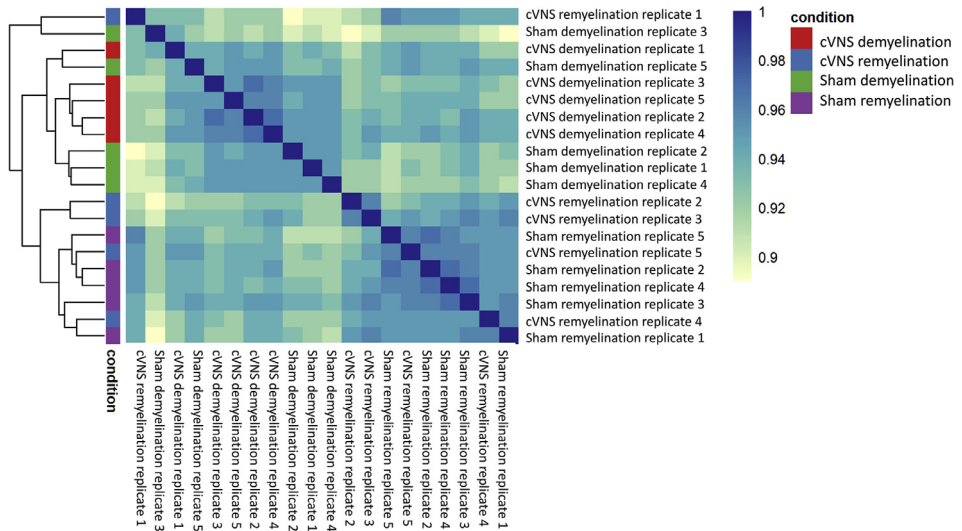


**Fig. 2.** Between-sample correlation heatmap was constructed using hierarchical clustering of Spearman correlation coefficients between protein expression values of all pairs of samples ( $n = 20$ ).

Differential expression of the quantified proteins was analyzed between cVNS and sham in the demyelination samples (**DE\_cVNS\_vs\_DE\_sham.txt**), and in the remyelination samples (**RE\_cVNS\_vs\_RE\_sham.txt**), and analogously between demyelination and remyelination in the cVNS (**DE\_cVNS\_vs\_RE\_cVNS.txt**), and in the sham samples (**DE\_sham\_vs\_RE\_sham.txt**). Statistical testing for differences between the two group means was performed, using the package limma [8]. Missing intensity values were imputed by randomly sampling from a normal distribution centered around each sample's noise level. Statistical significance for differential regulation was set with adjusted  $p$ -value ( $p\text{-adj}$ )  $\leq 0.05$  and  $|\log \text{fold changes (LFC)}| \geq 1$ . Volcano plots, visualizing the differential expression between experimental groups, are shown in Fig. 3. Heatmaps of Z-scored protein expression for immunologically and neurologically relevant proteins during demyelination and remyelination for the sham or VNS group are shown in Fig. 4.

## 4. Experimental Design, Materials and Methods

### 4.1. Experimental design

Female Lewis rats (7 weeks old) were implanted with a VNS electrode around the left cervical nerve [3]. After at least three weeks, they underwent stereotaxic injection with 1  $\mu\text{l}$  of 0.5 % LPC in the corpus callosum (1 mm caudal and 2 mm lateral to bregma, 2.5 mm ventral to brain surface) to induce a demyelinating lesion. Two days before the LPC injection, treatment with either cVNS (0.5 s ON/29.5 s OFF duty cycle, biphasic pulses, 1.0 mA intensity, 30 Hz frequency, 250  $\mu\text{s}$  pulse width) or sham was started and continued until 3 or 11 dpi. Sham treatment included the VNS electrode implantation and connection to the VNS set-up without the effective stimulation of the electrode. Rats were euthanized at 3 or 11 dpi for the demyelination or remyelination timepoint respectively, by an intraperitoneally administered overdose of sodium pentobarbital (600  $\text{mg kg}^{-1}$ , Vetoquinol, Belgium), followed by transcardiac perfusion with room temperature (RT) PBS and ice-cold PBS, and rapid brain isolation. Isolated brains were fixed in 4 % paraformaldehyde for 48 h, followed by cryoprotection with increasing sucrose solutions (10–20 % to 30 %) at 4  $^{\circ}\text{C}$ . Then, they were frozen in isopentane (2-methylbutane, Sigma-Aldrich) and liquid nitrogen ( $-196$   $^{\circ}\text{C}$ ) and stored in  $-80$   $^{\circ}\text{C}$ . In a subset of 20 animals, proteomics (LC–



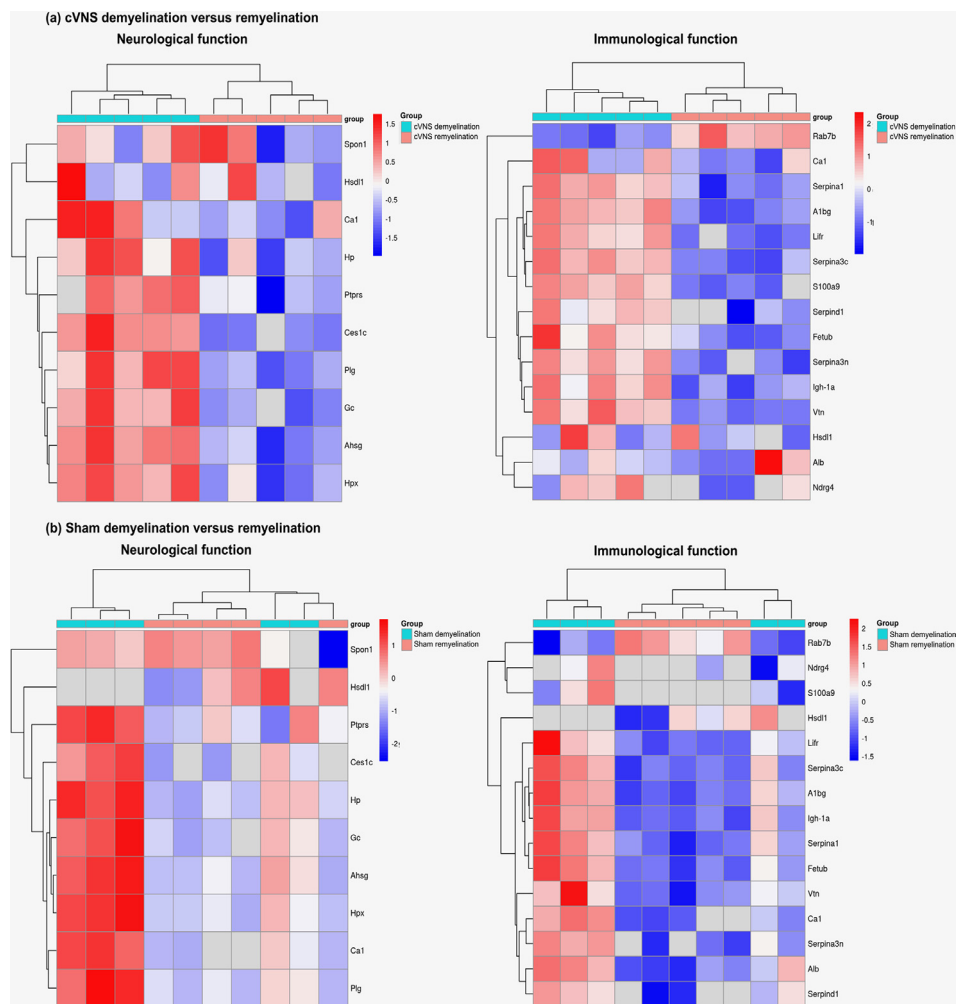


**Fig. 4.** Heatmap of Z-scored protein expression for a selection of immunologically and neurologically relevant proteins during demyelination and remyelination within the cVNS (a), or the sham group (b) (each experimental group  $n = 5$ ).

**Table 2**

Slices selected for proteomics.

Experimental groups	Demyelination experiment		Remyelination experiment	
	cVNS	Sham	cVNS	Sham
Samples	cVNS demyelination replicate 1	Sham demyelination replicate 1	cVNS remyelination replicate 1	Sham remyelination replicate 1
	cVNS demyelination replicate 2	Sham demyelination replicate 1	cVNS remyelination replicate 2	Sham remyelination replicate 2
	cVNS demyelination replicate 3	Sham demyelination replicate 1	cVNS remyelination replicate 3	Sham remyelination replicate 3
	cVNS demyelination replicate 4	Sham demyelination replicate 1	cVNS remyelination replicate 4	Sham remyelination replicate 4
	cVNS demyelination replicate 5	Sham demyelination replicate 1	cVNS remyelination replicate 5	Sham remyelination replicate 5
Total samples	$N = 5$	$N = 5$	$N = 5$	$N = 5$

saline (PBS), and the lesion was cut out and prepared for high-performance liquid chromatography coupled to tandem mass spectrometry (LC–MS/MS). To each sample 25  $\mu$ l lysis buffer containing 10 % sodium dodecyl sulfate (SDS) and 100 mM triethylammonium bicarbonate (TEAB), pH 8.5 was added and incubated at 50 °C overnight. Next, samples were transferred to a 96-well PIXUL plate and sonicated with a PIXUL Multisample sonicator (Active Motif) for 5 min with default settings (Pulse 50 cycles, PRF 1 kHz, Burst Rate 20 Hz). Samples were spun down shortly and incubated at 80 °C for 1 h. Then, sonication was repeated with the same settings for 6 min. After centrifugation of the samples for 15 min at maximum speed at RT to remove insoluble components, proteins were reduced by addition of 15 mM dithiothreitol and incubation for 30 min at 55 °C and then alkylated by addition of 30 mM iodoacetamide and incubation for 15 min at RT in the dark. Phosphoric acid was added to a final concentration of 2.75 % and subsequently samples were diluted 7-fold with binding buffer containing 90 % methanol in 100 mM TEAB, pH 7.55. After loading half of the samples to S-trap micro columns (Protifi) using centrifugation for 30 s at 4000 xg, the columns were washed once with 150  $\mu$ l binding buffer, three times with 150  $\mu$ l of a chloroform and methanol mixture (50/50, v/v) and twice with 150  $\mu$ l binding buffer. To each S-trap micro, 20  $\mu$ l 50 mM TEAB containing 1  $\mu$ g Trypsin was added for digestion overnight at 37 °C. Peptides were eluted in three times, first with 40  $\mu$ l 50 mM TEAB, then with 40  $\mu$ l 0.2 % formic acid (FA) in water and finally with 40  $\mu$ l 0.2 % FA in water/acetonitrile (ACN) (50/50, v/v). Eluted peptides were dried completely by vacuum centrifugation. All samples were redissolved in 20  $\mu$ l loading solvent A (0.1 % TFA in water/ACN (98:2, v/v)), diluted ten times in 0.1 % FA in water and 1/10th of the complete sample was loaded on Evtotips (Evosep, P/N EV2011) according to the manufacturer's instructions. All loaded Evtotips were stored in 0.1 % FA at 4 °C until LC–MS/MS analysis could be started.

#### 4.3. LC–MS/MS analysis

Samples were run in data-independent parallel accumulation serial fragmentation (DIA-PASEF) mode on an Evosep One LC-system (Evosep, Denmark) in-line connected to a timsTOF SCP (Bruker). Peptides were analyzed with the 20 SPD whisper method using the Aurora Gen3 Elite column (15 cm  $\times$  75  $\mu$ m I.D., 1.7  $\mu$ m beads, Evosep, Denmark), heated to 50 °C. Peptides were eluted from the column through the predefined 20SPD whisper gradient consisting of 0.1 % FA in LC–MS-grade water as solvent A and 0.1 % FA in ACN as solvent B. Eluting peptides were measured in positive polarity with a full-scan range of 100  $m/z$  to 1700  $m/z$ . The TIMS was operated at a fixed duty cycle close to 100 %, a ramp and accumulation time of 100 ms, ranging from  $1/KO = 0.64 \text{ Vscm}^2$  to  $1/KO = 1.50 \text{ Vscm}^2$ . Collision energy was linearly ramped as a function of the inverse mobility from 20 eV at  $1/KO = 0.60 \text{ Vscm}^2$  to 59 eV at  $1/KO = 1.60 \text{ Vscm}^2$ . A DIA-PASEF mass range of 400 Da to 1000 Da was used in a mobility range of  $1/KO = 0.64 \text{ Vscm}^2$  to  $1/KO = 1.37 \text{ Vscm}^2$  using a window size of 25 Da according to Table 3, resulting in a cycle time of 0.96 s.

#### 4.4. Data-analysis and statistics

Processing of raw proteomics data was performed by the VIB Proteomics Core using an in-house script. The code cannot be made publicly available, but a step-by-step overview is provided here. LC–MS/MS runs of all samples were searched using the DiaNN algorithm (version 1.8.1), library free. Spectra were searched against the *Rattus norvegicus* (TaxID: 10116) protein sequences in the Uniprot database (database release version of 06\_2023), containing 47,942 sequences ([www.uniprot.org](http://www.uniprot.org)). Enzyme specificity was set as C-terminal to arginine and lysine, also allowing cleavage at proline bonds with a maximum of two missed cleavages. Variable modifications were set to oxidation of methionine residues and acetylation of protein N-termini, fixed modification was set to carbamidomethylation of Cysteine residues. Mainly default settings were used, except for the addition of a 400–1000  $m/z$  precursor mass range filter and MS1 and MS2 mass tolerance was set to 15 and 20 ppm respectively.

**Table 3**  
dia-PASEF windows.

Cycle Id	Start IM [1/K0]	End IM [1/K0]	Start Mass [m/z]	End Mass [m/z]
1	0.64	0.83	400	425
2	0.64	0.85	425	450
3	0.64	0.87	450	475
4	0.64	0.9	475	500
5	0.64	0.92	500	525
6	0.64	0.94	525	550
7	0.64	0.97	550	575
8	0.64	0.99	575	600
1	0.83	1.01	600	625
2	0.85	1.04	625	650
3	0.87	1.06	650	675
4	0.9	1.09	675	700
5	0.92	1.11	700	725
6	0.94	1.13	725	750
7	0.97	1.16	750	775
8	0.99	1.18	775	800
1	1.01	1.37	800	825
2	1.04	1.37	825	850
3	1.06	1.37	850	875
4	1.09	1.37	875	900
5	1.11	1.37	900	925
6	1.13	1.37	925	950
7	1.16	1.37	950	975
8	1.18	1.37	975	1000

Further data analysis of the shotgun results was performed using R programming language, version 4.2.2. Protein expression matrices were prepared as follows: the DIA-NN main report output table was filtered at a precursor and protein library q-value cut-off of 1 % and only proteins identified by at least one proteotypic peptide were retained. After pivoting into a wide format, iBAQ intensity columns were then added to the matrix using the DIAgui's R package `get_IBAQ` function [9]. PG.MaxLFQ intensities were log<sub>2</sub> transformed and replicate samples were grouped. Proteins with less than three valid values in at least one group were removed and missing values were imputed from a normal distribution centered around the detection limit (package DEP) [10] leading to a list of 8172 quantified proteins in the experiment, used for further data analysis. A Principal Component Analysis (PCA) was performed on the replicate samples using all quantified proteins as variables, shown in Fig. 1, to visualize the intra- and inter-group replicate differences.

All further statistical analyses were performed using the script 'Data\_in\_brief.R', which has been uploaded to GitHub. Statistical analyses were performed using log<sub>2</sub>-transformed, imputed PG.MaxLFQ intensities in R. Samples were grouped based on treatment and condition and contrasts were defined as follows: DE\_cVNS\_vs\_DE\_sham = DE.cVNS - DE.sham (**DE\_cVNS\_vs\_DE\_sham.txt**), RE\_cVNS\_vs\_RE\_sham = RE.cVNS - RE.sham (**RE\_cVNS\_vs\_RE\_sham.txt**), DE\_cVNS\_vs\_RE\_sVNS = DE.cVNS - RE.cVNS (**DE\_cVNS\_vs\_RE\_cVNS.txt**), DE\_sham\_vs\_RE\_sham = DE.sham - RE.sham (**DE\_sham\_vs\_RE\_sham.txt**). Between-sample correlation heatmaps were constructed using hierarchical clustering of Spearman correlation coefficients. A heatmap of sample correlations after hierarchical clustering visualized correlation between protein expression of all pairs of samples (Fig. 2). Differentially expressed proteins were identified using limma [7] with empirical Bayes procedure and p-values corrected using Benjamini & Hochberg's procedure  $p\text{-adj} \leq 0.05$  and  $|LFC| \geq 1$ , shown in Fig. 3. A selection of inflammatory and neurological relevant differentially expressed proteins between demyelination and remyelination timepoints are highlighted on the volcano plots in Fig. 3, and shown in the heatmaps in Fig. 4.

The results and scientific discussion associated with this article can be found, in the online version, at [10.1016/j.j.brs.2024.04.012](https://doi.org/10.1016/j.j.brs.2024.04.012).

## Limitations

The use of only female rats in this dataset is a significant limitation because remyelination processes and responses by various brain cells can differ between males and females, potentially leading to biased results. Gonadal hormones may also impact these processes, further influencing outcomes, making it essential to consider sex differences in such studies.

## Ethics Statement

Experiments complied with the ARRIVE guidelines and were carried out according to European guidelines (Directive 2010/63/EU). Ethical approval was obtained by the animal ethics committee of Ghent University's Faculty of Medicine and Health Sciences (ECD 20/22).

## Data Availability

[PXD050858 \(Original data\)](#) (ProteomeXchange Consortium via the PRIDE partner repository).

## CRediT Author Statement

**Helen Bachmann:** Investigation, Writing – original draft, Visualization, Project administration; **Boris Vandemoortele:** Formal analysis, Visualization, Writing – review & editing; **Vanessa Vermeirssen:** Supervision, Conceptualization, Writing – review & editing; **Evelien Carrette:** Supervision; **Kristl Vonck:** Supervision, Writing – review & editing; **Paul Boon:** Supervision; **Robrecht Raedt:** Supervision, Resources, Writing – review & editing; **Guy Laureys:** Supervision, Conceptualization, Writing – review & editing, Funding acquisition.

## Acknowledgments

The authors thank the Ghent Light Microscopy CORE, the VIB Proteomics CORE, the Biobank of the University Ghent Hospital and in particular Anne-Sophie Bultinck and Eline Van Severen in supporting this paper. Helen Bachmann is a fellow of the Research Foundation Flanders (FWO) (1S25620N), funding was provided by the Charcot Research Fund (<https://www.fondation-charcot.org/>). These funding agencies were not involved in the study design, data collection, analysis, writing, and submission of the paper.

## Declaration of Competing Interest

The authors declare the following financial interests/personal relationships which may be considered as potential competing interests: Kristl Vonck received consultancy fees from LivaNova Europe and Synergia Medical. Paul Boon received consultancy fees from Livanova Europe. Helen Bachmann, Boris Vandemoortele, Vanessa Vermeirssen, Evelien Carrette, Robrecht Raedt, Guy Laureys have nothing to disclose.

## References

- [1] H. Bachmann, B. Vandemoortele, V. Vermeirssen, E. Carrette, K. Vonck, P. Boon, et al., Vagus nerve stimulation enhances remyelination and decreases innate neuroinflammation in lysolecithin-induced demyelination, *Brain Stimul.* 17 (2024) 575–587, doi:[10.1016/j.brs.2024.04.012](https://doi.org/10.1016/j.brs.2024.04.012).
- [2] M.B. Keough, S.K. Jensen, V. Wee Yong, Experimental demyelination and remyelination of murine spinal cord by focal injection of lysolecithin, *J. Vis. Exp.* 2015 (2015), doi:[10.3791/52679](https://doi.org/10.3791/52679).
- [3] R. El Tahry, L. Mollet, R. Raedt, J. Delbeke, V. De Herdt, T. Wyckhuys, et al., Repeated assessment of larynx compound muscle action potentials using a self-sizing cuff electrode around the vagus nerve in experimental rats, *J. Neurosci. Methods* 198 (2011) 287–293, doi:[10.1016/j.jneumeth.2011.04.007](https://doi.org/10.1016/j.jneumeth.2011.04.007).
- [4] W. Van Lysebettens, K. Vonck, L.E. Larsen, L. Stevens, C. Bouckaert, C. Germonpré, M. Sprengers, E. Carrette, J. Delbeke, W.J. Wadman, P. Boon, R. Raedt, Identification of vagus nerve stimulation parameters affecting rat hippocampal electrophysiology without temperature effects, *Brain Stimul.* 13 (5) (2020) 1198–1206, doi:[10.1016/j.brs.2020.05.011](https://doi.org/10.1016/j.brs.2020.05.011).
- [5] V. Schultz, F. van der Meer, C. Wrzos, U. Scheidt, E. Bahn, C. Stadelmann, et al., Acutely damaged axons are remyelinated in multiple sclerosis and experimental models of demyelination, *Glia* 65 (2017) 1350–1360, doi:[10.1002/glia.23167](https://doi.org/10.1002/glia.23167).
- [6] J.E. Merrill, In vitro and in vivo pharmacological models to assess demyelination and remyelination, *Neuropsychopharmacology* 34 (2009) 55–73, doi:[10.1038/npp.2008.145](https://doi.org/10.1038/npp.2008.145).
- [7] A. Mouihate, S. Kalakh, Ganaxolone enhances microglial clearance activity and promotes remyelination in focal demyelination in the corpus callosum of ovariectomized rats, *CNS Neurosci. Ther.* 26 (2020) 240–250, doi:[10.1111/cns.13195](https://doi.org/10.1111/cns.13195).
- [8] M.E. Ritchie, B. Phipson, D. Wu, Y. Hu, C.W. Law, W. Shi, et al., limma powers differential expression analyses for RNA-sequencing and microarray studies, *Nucleic Acids Res.* 43 (2015) e47, doi:[10.1093/nar/gkv007](https://doi.org/10.1093/nar/gkv007).
- [9] Gerault M.-A. DIAGui: dIAGui package n.d. <https://rdrr.io/github/mgerault/DIAGui/man/DIAGui.html> (accessed 13 December 2023).
- [10] X. Zhang, A.H. Smits, G.B.A. Van Tilburg, H. Ovaa, W. Huber, M. Vermeulen, Proteome-wide identification of ubiquitin interactions using UbIA-MS, *Nat. Protoc.* 13 (2018) 530–550, doi:[10.1038/NPROT.2017.147](https://doi.org/10.1038/NPROT.2017.147).